ISSN 1063-7834, Physics of the Solid State, 2013, Vol. 55, No. 10, pp. 2173–2181. © Pleiades Publishing, Ltd., 2013.
Original Russian Text © E.V. Lutsenko, N.V. Rzheutskii, V.N. Pavlovskii, G.P. Yablonskii, D.V. Nechaev, A.A. Sitnikova, V.V. Ratnikov, Ya.V. Kuznetsova, V.N. Zhmerik, S.V. Ivanov, 2013, published in Fizika Tverdogo Tela, 2013, Vol. 55, No. 10, pp. 2059–2067.

PROCEEDINGS OF THE THIRD ALL-RUSSIAN SYMPOSIUM "SEMICONDUCTOR LASERS: PHYSICS AND TECHNOLOGY"
(St. Petersburg, Russia, November 13–16, 2012)

Spontaneous and Stimulated Emission in the Mid-Ultraviolet Range of Quantum-Well Heterostructures Based on AlGaN Compounds Grown by Molecular Beam Epitaxy on *c*-Sapphire Substrates

E. V. Lutsenko[a, *], N. V. Rzheutskii[a], V. N. Pavlovskii[a], G. P. Yablonskii[a], D. V. Nechaev[b], A. A. Sitnikova[b], V. V. Ratnikov[b], Ya. V. Kuznetsova[b], V. N. Zhmerik[b], and S. V. Ivanov[b]

[a] *Stepanov Institute of Physics, National Academy of Sciences of Belarus, pr. Nezavisimosti 68, Minsk, 220072 Belarus*
** e-mail: e.lutsenko@ifanbel.bas-net.by*

[b] *Ioffe Physical-Technical Institute, Russian Academy of Sciences, Politekhnicheskaya ul. 26, St. Petersburg, 194021 Russia*

Abstract—This paper reports on the results of investigations of the spontaneous and stimulated luminescence in AlGaN heterostructures with a single quantum well and a high Al content (up to ~80 mol % in barrier layers), which were grown by plasma assisted molecular beam epitaxy (PAMBE) on *c*-sapphire substrates. It has been demonstrated that the stimulated emission occurs in the mid-ultraviolet range of the spectrum at wavelengths of 259, 270, and 289 nm with threshold excitation power densities of 1500, 900, and 700 kW/cm^2, respectively. It has been shown that there exists a possibility of TE polarization ($\mathbf{E} \perp \mathbf{c}$) of both stimulated and spontaneous luminescence down to wavelengths of 259 nm.

DOI: 10.1134/S106378341310020X

1. INTRODUCTION

Lasers operating in the ultraviolet (UV) range have been widely used in spectral analysis of various substances and media both for research purposes and for the solution of practical problems (for example, for the detection of life-threatening chemical and biological agents). These lasers are needed for the use in a wide range of biomedical applications, the development of new systems of hidden anti-interference UV optical communication, etc. [1]. The use of semiconductor UV laser sources instead of gaseous and solid-state UV lasers will increase the efficiency, reliability, and compactness of the aforementioned systems, expand their capabilities, and decrease the cost. The most promising for producing semiconductor laser sources in the subbands UV-*A*, UV-*B*, and, for the most part, UV-*C* (down to the minimum wavelength of ~214 nm) are wide-band-gap nitride compounds AlGaN with a continuously tunable band gap in the range from 3.4 (GaN) to 6.1 eV (AlN). However, the minimum wavelength of UV injection lasers, achieved in 2008, is equal to 336 nm [2], whereas shorter wavelength laser radiation is generated, as a rule, by optical pumping. The stimulated emission with a wavelength λ = 214 nm was achieved by pulsed optical pumping with a threshold optical power density of 9 MW/cm^2 in a bulk AlN layer on the *c*-Al_2O_3 substrate [3]. Recently, it was reported that enhanced spontaneous photoluminescence (PL) was excited in the range of 235–250 nm by electron beam pumping of AlGaN/AlN heterostructures [4]. However, for laser emission from AlGaN heterostructures with quantum wells (QWs) grown by different methods on *c*-sapphire or 4*H*-SiC substrates, the majority of research groups have used optical pumping, which has made it possible to observe lasing and stimulated emission in PL spectra in the wavelength range of 303–241 nm with threshold optical power densities of 0.8–1.3 MW/cm^2, respectively [5, 6]. A significantly lower value of the latter parameter (126 kW/cm^2) was achieved in 2011 for lasing at a wavelength of 267 nm in a heterostructure with multiple AlGaN quantum wells, grown on a single-crystal AlN substrate with a threading dislocation density of ~10^5 cm^{-2} [7]. Unfortunately, the mass use of such substrates is limited because of their high cost, and the development of technologies for growing AlGaN heterostructures on hetero-epitaxial substrates (as a rule, *c*-Al_2O_3) remains an urgent and important problem. Furthermore, it is necessary to develop methods for improving the efficiency of radiative recombination in such structures with a threading dislocation density up to ~10^9 cm^{-2}.

An extremely important problem associated with heterostructures based on AlGaN layers with a high Al content is the reconstruction of the valence band with an increase in the Al content, which leads to a change in the type of the upper hole subband [8–10]. For relaxed AlGaN layers with a low Al content (less than 25 mol %, band gap $E_g < 4.1$ eV), the upper position is occupied by the subband of heavy holes, which is responsible for dominant TE-polarization of PL with $\mathbf{E} \perp \mathbf{c}$. In case of a higher Al content (above 25 mol %),

Parameters of the heterostructures with $Al_xGa_{1-x}N/Al_yGa_{1-y}N$ single quantum wells

Parameter	Structure		
	no. 1	no. 2	no. 3
Growth temperature of the AlN nucleation layer, °C	570	790	790
Parameters of the AlN buffer layer:			
Layer thickness, μm	1.0	2.4	1.2
Thickness (nm)/number of GaN inserts	3.5/2	3.5/2	No
$\{AlGaN/AlN\}_{20}$ superlattice after the AlN buffer layer	Exists	Exists	No
Parameters of the bounding layer:			No
Specified Al content	0.85	0.85	–
Thickness, nm	300	1100	–
Thickness of the barrier layer, nm	120	100	110
Al content of barrier layers (y) according to:			
ratio of the calibrated flows	0.58	0.70	0.80
XRSMA measurements	0.60	0.73	0.78
XRD measurements under the assumption of complete relaxation of elastic stresses	0.60	0.71	0.63
Difference between the Al content in the barrier layer and the average Al content in the quantum wells ($y - x$)	0.1	0.1	0.1
Quantum well thickness, nm	3.0	2.3	2.1

the upper position is occupied by the spin–orbit split-off subband, which leads to dominant TM-polarization of PL with the electric field vector directed parallel to the c axis ($\mathbf{E} \parallel \mathbf{c}$). This polarization is highly undesirable for device structures, because the emission output with such a polarization from the active region of the structures in the directions perpendicular to the (0001) plane of the substrate (sapphire) is impossible. Moreover, the coefficients of reflection from the surfaces of a Fabry–Pérot cavity, formed by the cleaved facets, in a laser stripe design for radiation with TM-polarization are less than the corresponding coefficients for radiation with $\mathbf{E} \perp \mathbf{c}$ [11], which deteriorates the threshold characteristics of lasers [12].

The whole complex of the problems described above leads to the fact that the efficiency of light-emitting devices based on AlGaN is significantly (by more than an order of magnitude) inferior to similar devices based on InGaN heterostructures, and it is still problematic to achieve low-threshold lasing in the mid-UV region with a wavelength $\lambda < 300$ nm.

In this work, we have investigated the spectral and polarization characteristics of the spontaneous and stimulated luminescence in the wavelength range of 255–289 nm in heterostructures with quantum wells based on the AlGaN solid solutions with a high Al content (40–80 mol %), which were grown by plasma assisted molecular beam epitaxy (PAMBE) on c-sapphire substrates.

2. SAMPLE PREPARATION AND EXPERIMENTAL TECHNIQUE

The AlGaN heterostructures grown by the PAMBE method on sapphire (0001) substrates (the detailed description is given in our previous papers [5, 13–16]). The parameters of the three studied structures are presented in the table. The AlN buffer layers with a thickness ranging from 1.0 to 2.4 μm were grown at relatively high substrate temperatures $T_s \sim 780$°C and under the Al-rich conditions. The pulse supply of Al with a continuous nitrogen flow was used to prevent the formation of metallic microdroplets on the growth surface [14]. In addition, two strained GaN layers with a thickness of 3.5 nm and superlattices (SLs) $\{Al_{0.85}Ga_{0.15}N(5\text{ nm})/AlN(5\text{ nm})\}_{20}$ with an average Al content of 90 mol % were inserted into the buffer layers of samples nos. 1 and 2. Then, above the superlattices in samples nos. 1 and 2, bounding AlGaN layers with the same Al content (85 mol %) and thicknesses of 300 and 1100 nm, respectively, were grown. The upper barrier (waveguide) $Al_yGa_{1-y}N$ layers with different Al contents ($y = 0.58$–0.80) and approximately the same thickness for all samples (100–120 nm) were grown at a temperature $T_s \sim 700$°C under the metal-rich conditions near the threshold of the beginning of the formation of metallic (Ga) drops, as was described in detail in [15]. Under these conditions, the Al content in the bounding and barrier AlGaN layers was determined by the ratio of the calibrated flows of aluminum and activated nitrogen [16]. Single quantum wells (SQWs) $Al_xGa_{1-x}N/Al_yGa_{1-y}N$ ($y - x = 0.1$)

were formed by means of discrete submonolayer epitaxy and arranged asymmetrically in the waveguide, which, as was shown in [5], provided their spatial coincidence with the maximum of the electromagnetic wave field distribution in the waveguide.

The flows of the growth elements for the determination of the composition of AlGaN layers were calibrated using in situ laser reflectometry measurements of the growth rates of the layers under different stoichiometric conditions. The Al content was also controlled by post-growth measurements using the X-ray spectral microanalysis (XSMA) and X-ray diffraction (XRD) analysis. The structure and morphology of the samples were monitored by the in situ reflection high-energy electron diffraction (RHEED) method and, after the growth, analyzed using XRD, scanning electron microscopy (SEM), atomic force microscopy (AFM), and transmission electron microscopy (TEM).

Photoluminescence was excited by the fourth and fifth harmonic radiation from a Lotis Tii LS-2134 Nd : YAG laser with wavelengths of 266 and 213 nm, respectively, a pulse repetition rate of 15 Hz, and a pulse duration of 12 ns. The normally incident light with a maximum power density of ~10 MW/cm^2 was focused by a cylindrical lens onto the sample surface and had the form of a streak 60 μm wide. The excitation level was changed using a gradient attenuator. The luminescence spectra were recorded on a spectrometer equipped with a CCD line array (Hamamatsu) with a high linearity over a wide dynamic range of sensitivity. The PL spectra were taken from both the surface and the end face of the heterostructures. The measurements of PL polarization spectra from the end face of the heterostructure were carried out with the use of a Glan prism placed in front of the optical input of the spectrometer. All the optical measurements were performed at room temperature with spectral instruments calibrated against the wavelengths and spectral sensitivity in each particular configuration.

3. EXPERIMENTAL RESULTS AND DISCUSSION

The investigations of the structures with the use of different microscopic techniques have revealed sharp planar boundaries between regions with different compositions in all the studied samples, which is illustrated in Fig. 1. This figure shows the SEM and TEM images of some of the studied samples. The TEM images of all the structures demonstrate the presence of single quantum wells in waveguide layers. Moreover, the analysis of the TEM images also made it possible to investigate the behavior of threading dislocations, which are the major defects in the AlGaN heterostructures.

Figure 1c shows one of the general TEM images obtained for sample no. 1 under the diffraction conditions with the wave vector $g = (0002)$. From the analysis of this image it follows that the majority of dislocations are generated at the AlN/c-Al_2O_3 interface boundary, where their concentration is higher than 10^{11} cm^{-2}. However, the use of the optimized initial growth conditions described in [5] and the insertion of elastically strained thin GaN layers into the AlN buffer layers resulted in an increase in the probability of deviating both screw and edge dislocations from the vertical direction of their propagation. This led to the stop of propagation of dislocations, as well as to their coalescence or annihilation, which eventually provided a gradual decrease in the concentration of dislocations toward the upper active regions (waveguide layers) of the heterostructures.

Furthermore, we have recently shown that the concentration of dislocations can be further decreased by using high-temperature ($T_s = 790$°C) epitaxy with an enhanced migration for the growth of an AlN nucleation layer. This makes it possible to limit the generation of threading dislocations at the very early stages of growth at the expense of an increase in the size of nucleation blocks [13]. The conclusion about the significant decrease in the concentration of dislocations (especially in the early stages of growth) is confirmed by comparing Figs. 1c and 1d, which present the general TEM images of samples nos. 1 and 2, respectively, with the nucleation layers grown under different conditions. However, in the upper (barrier) layers, the difference between the concentrations of dislocations was not so large. According to the TEM evaluations, in sample no. 2 of the best quality in the studied series of structures, the densities of vertical screw and edge dislocations did not exceed 8×10^8 and 2×10^9 cm^{-2}, respectively, whereas in the other samples, these densities were approximately two times higher.

The results of the AFM examination of the surface morphology of the samples (not presented here) have confirmed the conclusions drawn from the analysis of the TEM images: the largest root-mean-square roughness rms = 1.45(2.19) nm was observed for areas $1 \times 1(10 \times 10)$ μm^2 in sample no. 1, whereas in sample no. 2, we obtained rms = 0.81(1.18) nm. The character of the morphology indicated a step-layer mechanism of growth in spirals around dislocations, and the larger roughness corresponded to a higher concentration of dislocations in the sample.

The spontaneous PL spectra were measured at an excitation power density of ~1 MW/cm^2 with the aim of decreasing the influence of the background concentration of equilibrium charge carriers on the luminescence intensity [17]. From a comparison of the spectra shown in Fig. 2, it follows that the most narrow single band with a half-width of ~10 nm at room temperature is observed in the PL spectrum of sample no. 1 with the minimum (in the studied series of samples) Al content in the waveguide layer ($y < 0.6$). The spectra of samples nos. 2 and 3 with a high Al content in this layer ($y > 0.7$) exhibit at least two overlapping broadened PL peaks: the short-wavelength peak can be tentatively attributed to the barrier layer PL, and the long-wave-

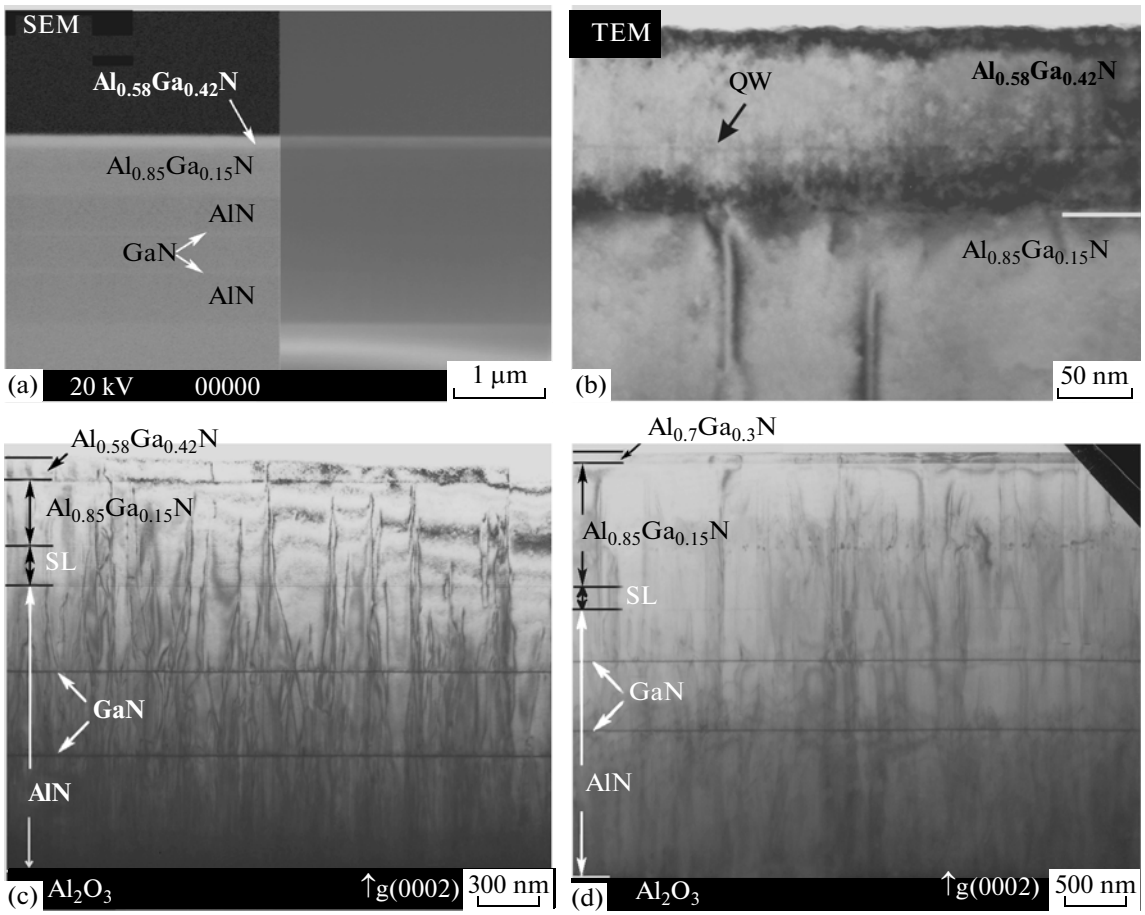

Fig. 1. (a) SEM images of the heterostructure of sample no. 1, obtained in the backscattered electron mode (left) and the secondary electron mode (right). (b) TEM image of the 2-nm-thick $Al_{0.58}Ga_{0.42}N$ barrier layer with $Al_{0.48}Ga_{0.52}N$ single quantum wells in the same structure and (c, d) general TEM images of the heterostructures in samples (c) no. 1 and (d) no. 2, obtained under diffraction conditions of the electron beam with the wave vector $\mathbf{g} = (0002)$.

length peak, to the quantum well PL. Smaller fluctuations in the PL intensity are likely to be associated with the superimposition of the interference pattern with the larger period in the structure of sample no. 3 with the smaller thickness. In the PL spectra presented in Fig. 2, also shown are the positions of the band gap edges of the waveguide layers $Al_yGa_{1-y}N$ (E_g^{AlGaN}), which were calculated according to the formula $E_g^{AlGaN}(y) = yE_g^{AlN} + (1-y)E_g^{GaN} + by(1-y)$ (by assuming the corresponding band gaps of the binary compounds to be $E_g^{AlN} = 6.08$ eV and $E_g^{GaN} = 3.42$ eV with the bowing parameter $b = 1.1$ [16]). The PL spectra observed in samples nos. 2 and 3 cover a substantially wider region (~60 nm), beginning from approximately the nominal band gap of the barrier layer; in this case, the Stokes shift of the PL peak of the barrier layer is ~400 meV for both samples. The obtained results indicate that the spontaneous PL of samples nos. 2 and 3 is determined by different localized states both in the $Al_yGa_{1-y}N$ ($y > 0.7$) barrier layers and in the quantum wells, and these states substantially overlap. Deep fluctuations of the potential relief in the AlGaN layers with a high Al content (more than 60 mol %), which are responsible for these localized states, can arise due to the heterogeneity of the composition of this ternary solid solution [18–21]. As a possible cause of this phenomenon, the authors considered the spontaneous formation of natural superlattice structures with a period of several monolayers in the layers with a high Al content [18]. Moreover, a local change in the potential relief in the AlGaN layers can be caused by the formation of Al- and Ga-rich regions due to the Ga diffusion toward threading dislocations and into the grain boundaries of the layer during the growth [19].

A comparison of the PL spectra with the structural properties of samples nos. 1 and 2 has demonstrated that threading dislocations and grain boundaries exert a relatively weak influence on the heterogeneity of the composition in the barrier layers. This follows from the fact that the broadest PL spectrum is observed in sample no. 2 (most structurally perfect in the studied series

of samples) with the lowest dislocation density and a relatively large grain size. Thus, the most probable cause of the observed broadening of the spontaneous PL spectra can be the spontaneous formation of a superlattice structure in the $Al_yGa_{1-y}N$ ($y > 0.6$) layers [18]. Detailed studies of this problem will be presented in a separate paper.

For all the studied heterostructures, the PL emission spectra taken from the end face of the sample with an increase in the excitation level undergo a narrowing with a superlinear increase in the intensity due to the stimulated PL. Figure 3 shows the PL spectra of all the heterostructures at different excitation levels and the dependences of the integrated intensity on the excitation level. The stimulated PL was observed at wavelengths of 289, 270, and 259 nm with threshold excitation power densities 700, 900, and 1500 kW/cm^2 for samples nos. 1–3, respectively.

For sample no. 1, the positions of the band maxima of the stimulated and spontaneous PL almost completely coincide with each other. This allows us to draw the conclusion about a relatively narrow distribution of localized energy states in the $Al_{0.48}Ga_{0.52}N/Al_{0.58}Ga_{0.42}N$ quantum well with a high density, which is also confirmed by the relatively small half-width of the spontaneous emission band. Furthermore, this heterostructure has a lower threshold of the stimulated emission as compared to the structures of samples nos. 2 and 3, which confirms the assumption about a higher homogeneity of the composition and thickness of the quantum well in this heterostructure.

In contrast to the structure of sample no. 1, the stimulated PL peak for samples nos. 2 and 3 is observed at the short-wavelength edge of the long-wavelength band of the spontaneous PL attributed by us to the quantum well emission in the spectral region of the tail of localized states in the barrier layer. This is probably associated with a more heterogeneous composition of the AlGaN compounds with an Al content of higher than 70 mol % due to the spontaneous formation of superlattices, which was assumed above. As a result, the tails of the density of states are broadened both in the barrier and in the quantum well. In addition, the quantum-confined Stark effect in wurtzite heterostructures with the (0001) orientation [22] should lead to an additional "smearing" of the spectrum and to an increase in the time of radiative recombination in the spectral region of the long-wavelength edge of the quantum well PL band. This prevents the development of the stimulated emission because of the low density of localized states and the low probability of radiative recombination due to the quantum-confined Stark effect. As a result, the optical gain in this spectral region is not enough to dominate over the loss and a significant enhancement of the spontaneous recombination occurs only in the short-wavelength region of the quantum well PL band. A similar position of the stimulated luminescence band and lasing was also observed by other authors in the heterostructures with the InGaN and AlGaN quantum wells [23–26].

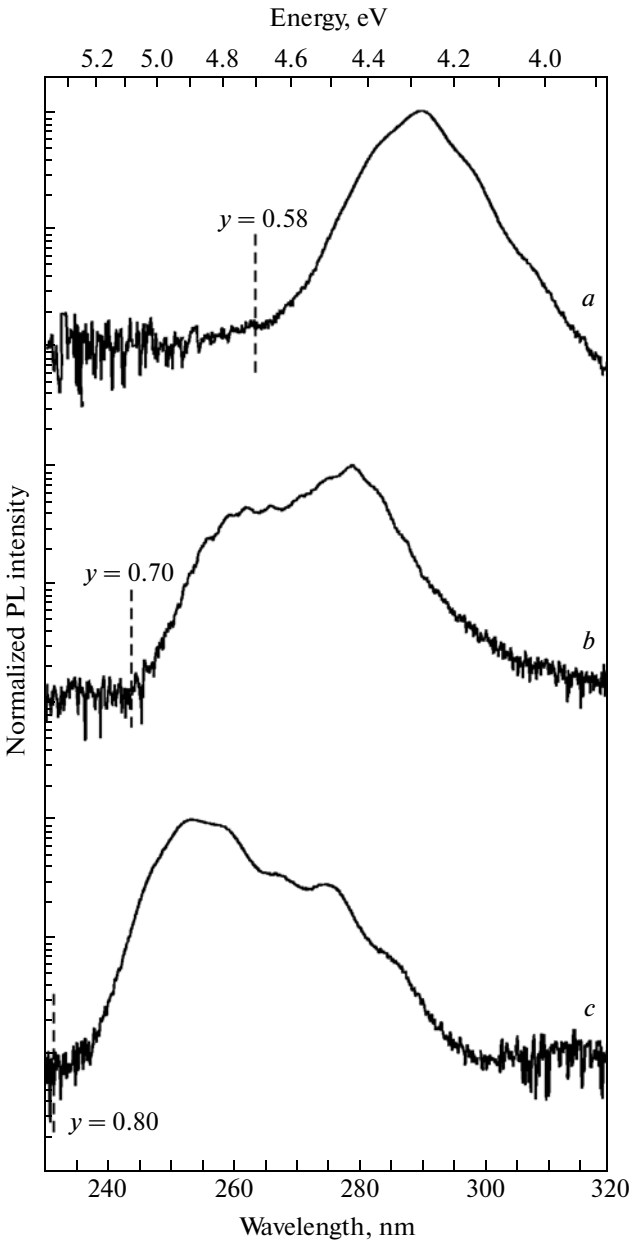

Fig. 2. PL spectra of the AlGaN heterostructures with quantum wells in samples (*a*) no. 1, (*b*) no. 2, and (*c*) no. 3, measured on the surface of the heterostructure at room temperature and an excitation power density of 1 MW/cm^2 (λ = 213 nm). Dashed lines indicate the energy positions corresponding to the expected values of the band gap (E_g) of the $Al_yGa_{1-y}N$ barrier layers with specified aluminum concentrations y.

The relatively high threshold excitation power density of the stimulated emission in sample no. 3 most likely is also associated with a higher concentration of threading dislocations in the active region of this structure due to the small thickness of the AlN buffer layer free of elastically strained GaN inserts and

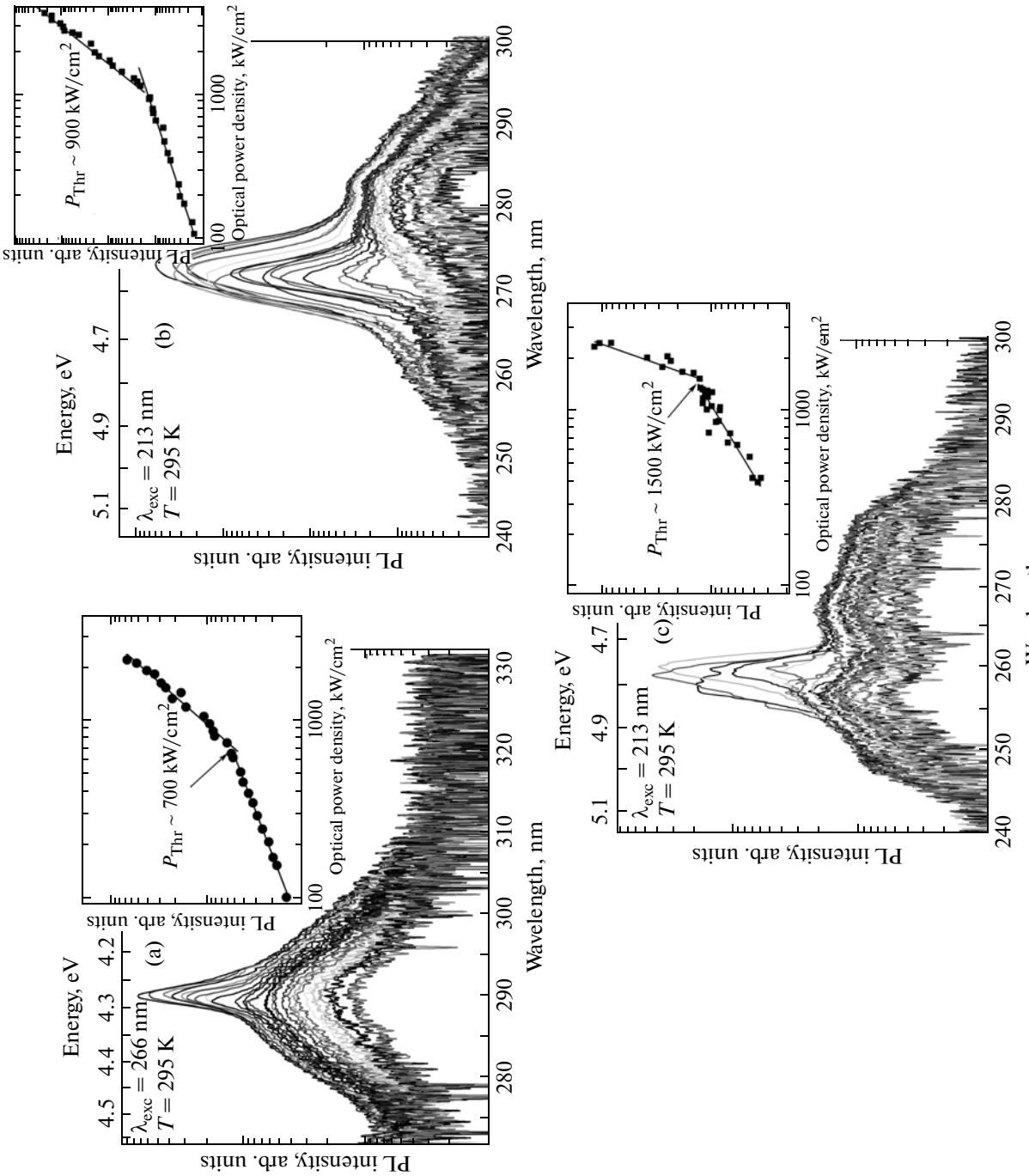

Fig. 3. PL spectra of the heterostructures of samples (a) no. 1, (b) no. 2, and (c) no. 3, measured from the end surface of the heterostructure at different excitation levels. The insets show the dependences of the integrated PL intensity on the excitation level, which were used to estimated the threshold power densities of the stimulated luminescence.

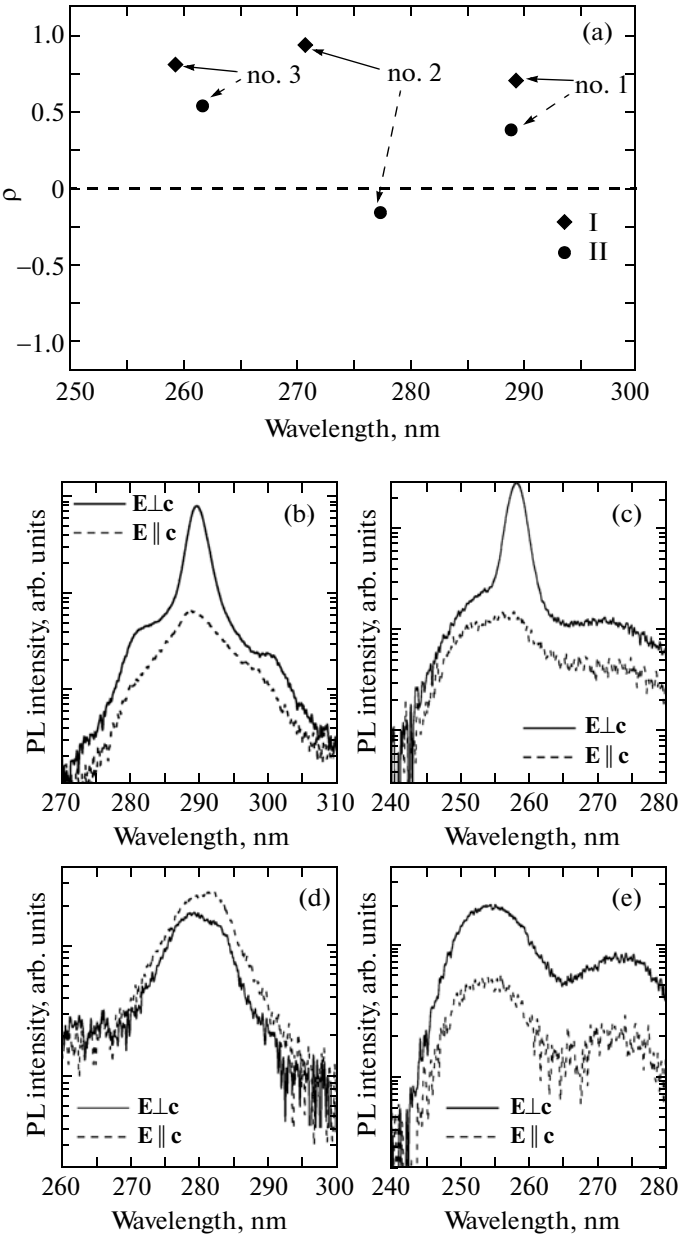

Fig. 4. (a) Degree of polarization ρ on the spectral position of the (I) stimulated PL band and (II) spontaneous PL band of the studied heterostructures upon excitation by laser radiation with a wavelength $\lambda = 213$ nm and power densities of ~2 MW/cm^2 (stimulated PL) and ~0.5 MW/cm^2 (spontaneous PL); (b, c) polarized spectra of stimulated PL in the heterostructures of samples (b) no. 1 and (c) no. 3; and (d, e) polarized spectra of spontaneous PL in the heterostructures of samples (d) no. 2 and (e) no. 3 under specified excitation conditions.

AlN/AlGaN superlattices, which limit the propagation of dislocations.

In the measurements of the polarization (**E** ⊥ **c** and **E** ∥ **c**) spectra of both the spontaneous and stimulated PL, the degree of polarization of the emission was estimated using the standard formula

$$\rho = \frac{(I_\perp - I_\parallel)}{(I_\perp + I_\parallel)}, \quad (1)$$

where $I_\perp$ and $I_\parallel$ are the integrated intensities of the PL bands polarized in the directions **E** ⊥ **c** (TE-polarization) and **E** ∥ **c** (TM-polarization), respectively. For the stimulated PL in all the heterostructures, the degree of polarization has positive relatively high values ($\rho \geq 0.7$), as is shown in Fig. 4a.

The stimulated emission spectra for all the studied samples (Figs. 4b and 4c show the spectra of samples nos. 1 and 3, respectively) have a significantly higher

intensity and a smaller half-width of the emission component with the TE polarization as compared to the TM-polarized component.

The degree of polarization of the spontaneous emission, in contrast to the stimulated emission, in the studied samples is different and takes on both positive values (in samples nos. 1 and 3) and a negative value (in sample no. 2 with the $Al_{0.7}Ga_{0.3}N$ waveguide layer) (Fig. 4a). The observation of the preferred TM polarization in the latter case corresponds to theoretical calculations and experimental results obtained by different authors for quantum wells (with $y - x = 0.1$) in the relaxed and weakly strained $Al_yGa_{1-y}N$ barrier layers with $y > 0.7$ [8–10]. Hence, the positive degree of polarization ($\rho = 0.5$) of the shortest wavelength spontaneous PL for the structure of sample no. 3 (Figs. 4a, 4e) with the maximum (in the studied series of samples) Al content in the waveguide layer ($y = 0.8$) was an unexpected result. This effect can be explained by the action of elastic stresses in the considered heterostructure, in which the calculated value of the compressive strain in the $Al_{0.78}Ga_{0.22}N$ barrier layer under the assumption of the pseudomorphic growth is $\varepsilon_{xx} = -0.55\%$. In the quantum well, the compressive stress is approximately 1.5 times higher ($\varepsilon_{xx} \sim -0.8\%$). These values of the strains correspond to theoretical estimates of the elastic stresses that are necessary to suppress the reconstruction of the valence band in the AlGaN quantum well heterostructures with a high Al content (above 70 mol % in the barrier layer), whereby it becomes possible to achieve the TE polarization of the spontaneous emission [9, 10]. It should be noted that, in these studies, the experimental confirmation of the calculations has so far served the observation of a positive degree of polarization ($\rho > 0.75$) of the emission with a wavelength of 253 nm from the AlGaN quantum well light-emitting diode heterostructure pseudomorphically grown on a homoepitaxial AlN substrate [9].

In sample no. 3 studied in this work, the pseudomorphic growth is confirmed by the significant difference between the Al content in the barrier layer, which was determined using the relative position of the XRD peak under the assumption of a complete relaxation of elastic stresses in the layer ($y = 0.63$), and the values of the layer composition obtained from the ratio of the flows of aluminum and activated nitrogen ($y = 0.8$) and the XRSMA data ($y = 0.78$). This difference indicates the existence of a compressive strain in the $Al_yGa_{1-y}N$ barrier layer. According to [27], the composition of this layer under the assumption of the pseudomorphic growth can be obtained using the expression

$$y = \frac{(1-\nu)}{(1+\nu)}\frac{(c_{\text{meas}}^{\text{AlGaN}} c_0^{\text{CaN}})}{(c_0^{\text{AlN}} - c_0^{\text{GaN}})}, \qquad (2)$$

where ν is the Poisson's ratio, whose exact value for AlGaN has not been determined, and, therefore, it was estimated from the value of $\nu = 0.20$ obtained by averaging the data of many studies on the experimental and theoretical determination of the elastic constants for the AlN and GaN layers, which were generalized in [27]; $c_{\text{meas}}^{\text{AlGaN}}$ is the lattice constant found in accordance with the positions of the peaks in the XRD rocking curve; and c_0^{AlN} and c_0^{GaN} are the lattice constants of the unstrained binary compounds AlN and GaN (4.981 and 5.185 Å, respectively, according to [28, 29]). By substituting these values into expression (2), we obtain the Al content in the layer $y = 0.75$, which is only slightly different from the XRSMA data ($y = 0.78$). This result confirms the high value of the compressive strain ($\varepsilon_{xx} < -0.5\%$) in sample no. 3 ($Al_{0.7}Ga_{0.3}N$(2.1 nm)/$Al_{0.8}Ga_{0.2}N$/AlN/$c$-$Al_2O_3$), which is the cause for the observed positive degree of polarization of the spontaneous PL in this structure.

It should be noted that the difference between the Al contents in the barrier layers, determined by different methods, is substantially smaller for samples nos. 1 and 2 (see table), which suggests a complete relaxation of elastic stresses in the upper layers of the structures. Indeed, these samples were grown using relatively thick AlN buffer layers with several inserts of thin GaN binary layers, i.e., AlGaN/AlN superlattices. The growth of the barrier layer in these samples was preceded by the growth of thick (~500 nm) bounding $Al_{0.85}Ga_{0.15}N$ layers. All these specific features decreased compressive stresses in the upper barrier layers, which was the cause for the observation of the negative degree of polarization of the spontaneous PL in sample no. 2. For sample no. 1, the positive degree of polarization of the spontaneous PL can be explained by the insufficient reconstruction of the valence band of $Al_{0.58}Ga_{0.42}N$ due to the lower aluminum concentration. A change in the direction of the preferred polarization of the PL emission of sample no. 2 with an increase in the excitation level above the threshold of the stimulated PL indicates that, in the enhanced PL mode, the direction of polarization of the PL emission is determined by the high reflectivity of the TE-mode.

4. CONCLUSIONS

The investigations of the spontaneous photoluminescence of heterostructures with single quantum wells based on the AlGaN ternary compounds with a high Al content (more than 60 mol %) and a concentration of threading dislocations in the range of 10^8–10^9 cm^{-2} have revealed a complex character of the spectra, which indicates radiative recombination through localized states in barrier layers and quantum wells. It has been found that the width of the photoluminescence spectrum is determined by the heterogeneity of the AlGaN composition in these layers, which

increases with an increase in the average aluminum concentration ($y > 0.7$).

It has been demonstrated that the stimulated luminescence occurs in the mid-UV range of the spectrum at wavelengths of 289, 270, and 259 nm in heterostructures with AlGaN single quantum wells grown on *c*-sapphire substrates with threshold optical excitation power densities of 700, 900, and 1500 kW/cm^2, respectively, which, at present, is the best result obtained for hetero-epitaxial semiconductor structures. For all the studied structures, the stimulated luminescence was polarized in the direction $\mathbf{E} \perp \mathbf{c}$, which is determined primarily by the high reflectivity of the TE-mode. The positive ($\mathbf{E} \perp \mathbf{c}$) degree of polarization $\rho = 0.5$ of the spontaneous photoluminescence of the heterostructure with $Al_{0.7}Ga_{0.3}N$(2.1 nm)/$Al_{0.8}Ga_{0.2}N$/AlN/*c*-Al_2O_3 quantum wells is explained by the effect exerted by elastic compressive stresses that restrict the reconstruction of the valence bands of the solid solution in the quantum wells.

ACKNOWLEDGMENTS

This study was supported by the Russian Academy of Sciences within the framework of the program "New Materials," the Russian Foundation for Basic Research (project no. 12-02-00865-a), and the King Abdulaziz City for Science and Technology (KACST) Project.

REFERENCES

1. H. Yoshida, Y. Yamashita, M. Kuwabara, and H. Kan, Nat. Photonics **2**, 551 (2008).
2. H. Yoshida, Y. Yamashita, M. Kuwabara, and H. Kan, Appl. Phys. Lett. **93**, 241106 (2008).
3. M. Shatalov, M. Gaevski, V. Adivarahan, and A. Khan, Jpn. J. Appl. Phys. **45**, L1286 (2006).
4. E. F. Pecora, W. Zhang, A. Yu. Nikiforov, L. Zhou, D. J. Smith, J. Yin, R. Paiella, L. D. Negro, and T. D. Moustakas, Appl. Phys. Lett. **100** (6), 061111 (2012).
5. V. N. Jmerik, A. M. Mizerov, A. A. Sitnikova, P. S. Kop'ev, S. V. Ivanov, E. V. Lutsenko, N. P. Tarasuk, N. V. Rzheutskii, and G. P. Yablonskii, Appl. Phys. Lett. **96**, 141112 (2010).
6. T. Takano, Y. Narita, A. Horiuchi, and H. Kawanishi, Appl. Phys. Lett. **84**, 3567 (2004).
7. T. Wunderer, C. L. Chua, J. E. Northrup, Z. Yang, N. M. Johnson, M. Kneissl, G. A. Garrett, H. Shen, M. Wraback, B. Moody, H. S. Craft, R. Schlesser, R. F. Dalmau, and Z. Sitar, Phys. Status Solidi C **9** (3–4), 822 (2012).
8. K. B. Nam, J. Li, M. L. Nakarmi, J. Y. Lin, and H. X. Jiang, Appl. Phys. Lett. **84** (25), 5264 (2004).
9. J. E. Northrup, C. L. Chua, Z. Yang, T. Wunderer, M. Kneissl, N. M. Johnson, and T. Kolbe, Appl. Phys. Lett. **100**, 021101 (2012).
10. M. V. Durnev and S. Yu. Karpov, Phys. Status Solidi B **250** (1), 180 (2013).
11. T. Ikegami, IEEE J. Quantum Electron. **QE-8**, 470 (1972).
12. H. Kawanishi, M. Senuma, and T. Nukui, Appl. Phys. Lett. **89**, 041126 (2006).
13. D. V. Nechaev, P. A. Aseev, V. N. Jmerik, P. N. Brunkov, Y. V. Kuznetsova, A. A. Sitnikova, V. V. Ratnikov, and S. V. Ivanov, J. Cryst. Growth (2013) (in press).
14. V. N. Jmerik, A. M. Mizerov, D. V. Nechaev, P. A. Aseev, A. A. Sitnikova, S. I. Troshkov, P. S. Kop'ev, and S. V. Ivanov, J. Crys. Growth **354**, 188 (2012).
15. A. M. Mizerov, V. N. Jmerik, P. S. Kop'ev, and S. V. Ivanov, Phys. Status Solidi C **7**, 2046 (2010).
16. V. N. Jmerik, A. M. Mizerov, T. V. Shubina, A. V. Sakharov, A. A. Sitnikova, P. S. Kop'ev, S. V. Ivanov, E. V. Lutsenko, A. V. Danil'chik, N. V. Rzheutskii, and G. P. Yablonskii, Semiconductors **42** (12), 1420 (2008).
17. E. V. Lutsenko, M. V. Rzheutski, V. Z. Zubialevich, V. N. Pavlovskii, G. P. Yablonskii, A. S. Shulenkov, I. Reklaitis, A. Kadys, T. Malinauskas, S. Nargelas, K. Jarašiūnas, and A. Žukauskas, Phys. Status Solidi C **10**, 511 (2013).
18. M. Gao, S. T. Bradley, Yu Cao, D. Jena, Y. Lin, S. A. Ringel, J. Hwang, W. J. Schaff, and L. J. Brillson, J. Appl. Phys. **100**, 103512 (2006).
19. A. Pinos, V. Liuolia, S. Marcinkevicius, J. Yang, R. Gaska, and M. S. Shur, J. Appl. Phys. **109**, 113516 (2011).
20. V. Fellmann, P. Jaffrennou, D. Sam-Giao, B. Gayral, K. Lorenz, E. Alves, and B. Daudin, Jpn. J. Appl. Phys. **50**, 031001 (2011).
21. E. Kuokstis, W. H. Sun, M. Shatalov, J. W. Yang, and M. A. Khan, Appl. Phys. Lett. **88**, 261905 (2006).
22. J. Mickevicius, E. Kuokstis, V. Liuolia, G. Tamulaitis, M. S. Shur, J. Yang, and R. Gaska, Phys. Status Solidi A **207**, 423 (2010).
23. A. Žukauskas, K. Kazlauskas, G. Tamulaitis, P. Pobedinskas, S. Juršėnas, S. Miasojedovas, V. Yu. Ivanov, M. Godlewski, C. Skierbiszewski, M. Siekacz, G. Franssen, P. Perlin, T. Suski, and I. Grzegory, Phys. Status Solidi B **243**, 1614 (2006).
24. J. Mickevicius, J. Jurkevicius, K. Kazlauskas, A. Zukauskas, G. Tamulaitis, M. S. Shur, M. Shatalov, J. Yang, and R. Gaska, Appl. Phys. Lett. **100**, 081902 (2012).
25. M. Strassburg, A. Hoffmann, J. Holst, J. Christen, T. Riemann, F. Bertram, and P. Fischer, Phys. Status Solidi C **0**, 1835 (2003).
26. G. P. Yablonskii, E. V. Lutsenko, V. N. Pavlovskii, I. P. Marko, A. L. Gurskii, V. Z. Zubialevich, A. V. Mudryi, O. Schon, H. Protzmann, M. Lunenburger, B. Schineller, and M. Heuken, Appl. Phys. Lett. **79**, 1953 (2001).
27. M. A. Moram and M. E. Vickers, Rep. Prog. Phys. **72**, 036502 (2009).
28. W. Paszkowicz, M. Knapp, S. Podsiado, G. Kamler, and G. B. Peka, Acta Phys. Pol. **101**, 781 (2002).
29. C. Kisielowski, J. Kruger, S. Ruvimov, T. Suski, J. W. Ager, III, E. Jones, Z. Liliental-Weber, M. Rubin, E. R. Weber, M. D. Bremser, and R. F. Davis, Phys. Rev. B: Condens. Matter **54**, 17745 (1996).

Translated by O. Borovik-Romanova